Engineering Journal issn: 0125-8281

Article

Lateral Loading Test of Reinforced Concrete Bored Pile in Stiff Clay and Near Slope

Wichairat Kaewjuea[1,a], Somboon Shaingchin[2,b,*], Wittawat Khamtip[2], Thanakorn Chompoorat[2], and Preeda Chaimahawan[2]

1 Department of Civil and Environmental Engineering, Faculty of Engineering, Prince of Songkla University, Songkhla 90110, Thailand
2 Department of Civil Engineering, Faculty of Engineering, University of Phayao, Phayao 56000, Thailand
E-mail: [a]kwichairat@eng.psu.ac.th, [b,*]somboon.sh@up.ac.th (Corresponding author)

Abstract. Staff residence of University of Phayao has been constructed near slope. The inhabitants in the residence are concerned about the lateral strength of the pile foundation during earthquake. This paper involves the evaluation of reinforced concrete bored piles of the residence under lateral loading. In field experiment, two full-scale bored piles were built near the slope of 1:1.5 adjacent to the residence. Two lateral load patterns that push the piles in and out were applied at the pile head. The maximum value of the lateral force was 65 kN representing the base shear force due to earthquake in Thailand. The test results show that the lateral displacements of the pile do not exceed 3 mm and stress in the longitudinal reinforcement is below the yield point. It is implied that the bored piles of staff residence can resist the lateral load imposed on the structure during an earthquake. For the analysis, the pile is modeled using frame elements and the surrounding soil is assigned by horizontal springs. The stiffness of springs is validated by comparing to the test results of the previous researches and this study. It is found that using the proper soil spring stiffness and flexural rigidity values in the structural pile analysis can capture elastic responses including the lateral displacement, bending moment and depth of inflection point.

Keywords: Pile foundation, lateral load test, full-scale test, earthquake.

ENGINEERING JOURNAL Volume 26 Issue 3
Received 17 August 2021
Accepted 1 March 2022
Published 31 March 2022
Online at https://engj.org/
DOI:10.4186/ej.2022.26.3.29

DOI:10.4186/ej.2022.26.3.29

1. Introduction

Foundation is the first part of any construction to support the structure to build upon. When the foundation is poorly designed or constructed, it can post a serious risk to the inhabitants and the neighborhood as a whole. Moreover, the repairing foundation problems are difficult, expensive and unpredictable because foundation is embedded in a soil medium. The most of these problems are rarely invisible and need professional foundation engineers to recognize and correct the problems. However, there are several methods to prevent the foundation problems. One of them is design the building foundation carefully by considering both primary loadings and secondary loadings.

Recently, Ministry of Interior (Thailand) issued Ministerial Regulation prescribing load capacity, resistance, and durability of buildings, and bearing capacity of soil supporting buildings in seismic resistance B.E. 2564 (2021) amended by the Building Control Act (No.5), B.E. 2558 (2015) [1]. As a result, structural designers have to consider effect from earthquake load to ensure stability of building structures and foundations. Earthquake causes damages in structures due to inertia forces which are created by ground accelerations. Therefore, foundation structures must be designed to resist both vertical and horizontal loads. The vertical load consists of dead load, live load and impact load. The horizontal load comprises of wind load and shearing force from earthquake.

Phayao province is one of twelve provinces classified in near fault zone (zone 3) according to Ministerial Regulation [1]. Public buildings, structures in educational institutions, buildings that have more than 3 storeys or have height from ten meters could be affected by earthquake. In addition, Phayao province located at northern part of Thailand that most regions are mountainous. Building constructions in Phayao province are sometimes on area of cut slope. For example, staff residence of Phayao University has been constructed on cut slope as seen in Fig. 1(a). The residence is 4-storeys reinforced concrete (RC) building, 11.55 meter in width, 61.20 meters in length. The foundation is bores pile system and the section of piles is shown in Fig. 1(b). All piles are the bored piles with 350 millimeters in diameter and 12 meters in depth. When the building officially opened, a large number of inhabitants moved into, the inhabitants in the residence are concerned about the lateral strength of the pile foundation during earthquake. Thus, the combination of primary load and earthquake load should be considered in order to investigate the ability of building especially the foundation of building near steep slope. That is the reason, it is necessary to conduct lateral load testing to confirm the capacity of the pile foundation and the test results are useful for comparison with the analysis model of the pile foundation.

(a) staff residence building

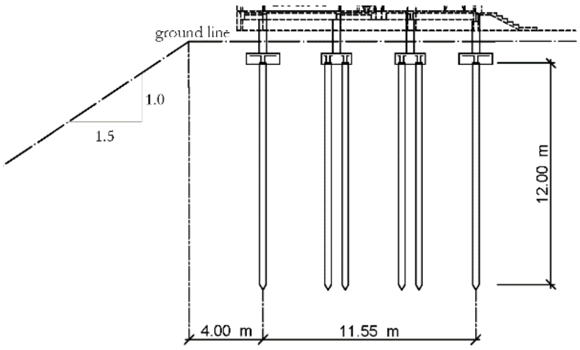

(b) section of piles in soil

Fig. 1. Staff residence of University of Phayao.

Many researchers studied the behavior of structural piles under lateral loading in the past and proposed the analysis methods for design pile foundation [2-3]. Some researches were parametric studies of piles subjected to lateral static and dynamic loadings using finite element method. The parameters that affect the pile behavior are pile diameter, pile spacing, number and arrangement of piles and soil properties [4-5]. However, there were a few researchers conducted full-scale experiment. The full-scale tests of piles under lateral loading usually were performed on site that piles would be constructed. For examples, Huang et al. [6] tested the full-scale groups of bored and driven piles under lateral load. The diameters of bored piles were 1.50 meters and the driven piles were hollow section, 0.80 meters outside diameter and 0.56 meter inside, with concrete infill. The depth of piles was 35 meters. Then, the numerical analysis using *p-y* model with the concept of *p* multiplier was performed to optimize the design of pile foundations for the proposed high-speed rail system in Taiwan. Hanich et al. [7] performed lateral load test on two full-scale bored piles to confirm the lateral load capacity of pile foundation of arch bridge across the Vardar River in Skopje, North Macedonia. The piles were 1.80 meters in diameter and 16.00 meters in length. The test results were proved that the foundation of the bridge could carry double of designed lateral load. Moreover, maximum displacement at the top of the pile was not to excess the designed displacement. Chaosittichai and Anantanasakul [8] presented the lateral load-displacement behavior of driven piles in soft Bangkok clay, Thailand. The computer program LPILE with Matlock's *p-y* model

[9] was also used to predict the plie behavior. The results indicated that the lateral load-displacement relations were slightly more than those of the tests. However, some factored values were employed to provide best fits of load-displacement relationships. The effects of slope on the behavior of pile foundation under lateral loading were studied in the past decade. Most researchers studied by small-scale model test at laboratory or finite element analysis [10-13]. It was found that the lateral load capacity of piles on the crest slope or on the sloping ground was reduced significantly compared to pile on horizontal ground. Nimityongskul et al. [14] performed full-scale tests to study the behavior of piles installed in cohesive soils and near slope. It was found that the slope significantly affects the lateral load capacity of piles installed less than 8 time of pile diameter from the slope crest. In addition, Nimityongskul et al. proposed the *p*-multipliers accounting for the slope effect.

As described, the results of full-scale test are used to validate the analysis methods and ensure the procedure to design pile foundation that is depended on the soil type and properties at construction site. In this study, full-scale lateral load tests and numerical simulations are carried to evaluate the response of reinforced concrete bored pile of staff residence in University of Phayao located near a steep slope. In the numerical model, influence of soil-structure interaction on response of bored piles subjected to lateral load is investigated using the equivalent spring stiffness to represent the surrounding soil that is commonly and acceptable method used to design pile foundation in Thailand [15].

2. Pile Specimens and Test Setup

In this study, two cast-in-place RC bored piles were constructed near slope beside the staff residence. Pile C1 was located 1 meter from crest slope with 1:1.5 of gradient and the distance between pile C1 and C2 was 3 meters as shown in Fig. 2. The details of bored-pile specimens were similar with the piles of staff residence. The diameter was 350 mm. Because the test was without vertical load, the depth of pile specimens was reduced to 7 meters. Six-deformed bars with diameter of 12 mm and grade SD40, a minimum yield strength not less than 390 MPa according to Thai Industrial Standards (TIS 24-2559) [16], were used for longitudinal reinforcement. Transverse reinforcement was spiral round bar with diameter of 6 mm and spacing at 150 mm with grade SR24, yield strength not less than 235 MPa (TIS 20-2559) [17].

It should be noted that there was a problem while drilling the borehole of C1. The drilling head wobbled when passing stiff soil layer (depth about at 1-2 meters). As a result, the actual diameter of the pile C1 before pouring concrete was 570 mm that was greater than that of the construction drawing as 350 mm. However, there was no problem with pile C2 while drilling. The reinforcement cage was prepared and placed in the bored hole. It should be at the center of hole but the center of the cage was moved from the center of bored hole about 27.5 mm during pouring concrete as sketched in Fig. 3. Therefore, the pile C1 was used only as support and the pile C2 was used to study the behavior of the lateral load on pile foundation.

The mechanical properties of concrete and reinforcing bars were determined by laboratory tests. The compressive strength of the pouring concrete cylinder standard was 36.8 MPa cured in water 28 days. The yielding strength of longitudinal reinforcement was 650.2 MPa.

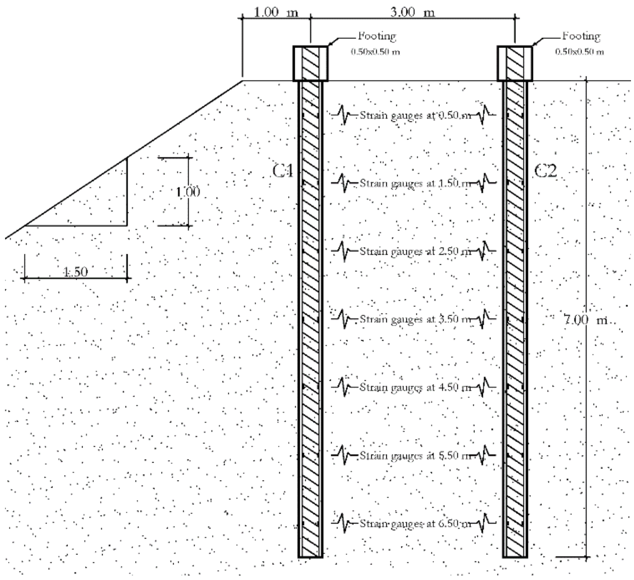

Fig. 2. Pile specimens.

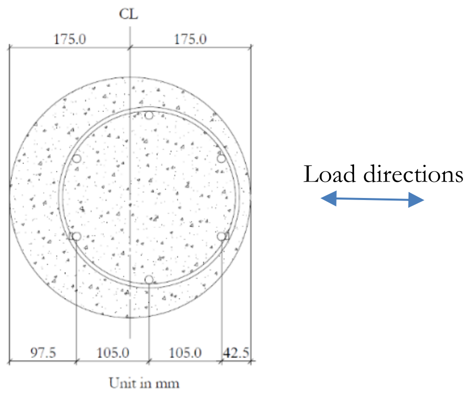

Fig. 3. Section details of pile C2.

The lateral load was applied to the pile heads by increasing the pressure on hydraulic jack through the bracing steel structures attached to the two piles. Load cell was also assembled to measure the lateral load. There are two patterns of applied lateral load. First, the hydraulic jack pushed the piles away from each another as shown in Fig. 4(a). Second, the hydraulic jack pushed on steel frame that makes the piles towards each other as seen in Fig. 4(b). In the next section, if the head of pile C2 moves to the right direction, the displacement is positive sign. The displacement in the opposite direction is negative value. The lateral displacement of pile head was recorded using displacement transducer. Strains of longitudinal

DOI:10.4186/ej.2022.26.3.29

reinforcement were measured using strain gauges that were attached directly to the reinforcement at depths of 0.50, 1.50, 2.50, 3.50, 4.50, 5.50 and 6.50 meters from the ground line. For each depth, two strain gauges were placed on opposite sides of the reinforcement to collect data for calculating the bending curvature of the section at each depth. All strain gauges were connected to a data logger which recorded the data every 0.5 second. Figure 5 shows the field test set up.

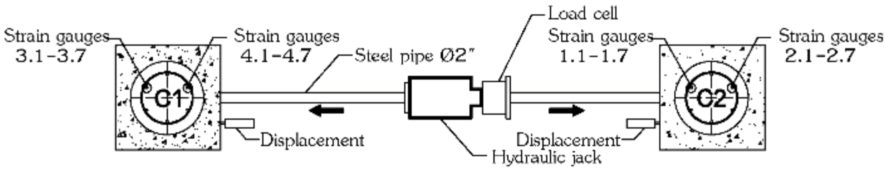

(a) Load pattern 1

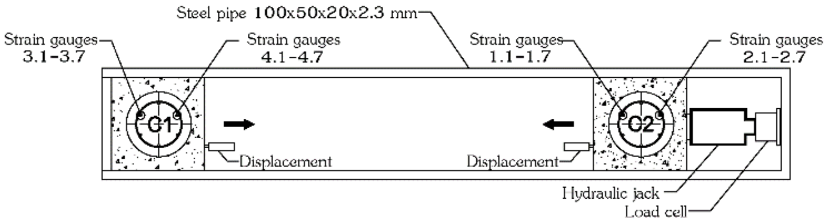

(b) Load pattern 2

Fig. 4. Lateral load test set up.

Fig. 5. Field test set up.

Ministry of Interior, Thailand issued Ministerial Regulation prescribing load capacity, resistance, and durability of buildings, and bearing capacity of soil supporting buildings in seismic resistance B.E. 2564 (2021) [1], the shear force at the base of structure is approximately 5% to 7% of the dead load. In this study, the maximum allowable vertical load of the pile is about 350 kN. If the lateral load is estimated at 7% of the vertical load, the allowable lateral load should be 24.5 kN. To calculate the maximum test load, the allowable load should be multiplied by the factor of safety. The safety factor in geotechnical engineering is about 2.5. Hence, the maximum test load in this study is 65 kN.

3. Test Results

Relationships between lateral load and pile head displacement of the piles C1 and C2 are presented in Figs. 6 and 7. The lateral displacement of pile gradually increases with increasing the applied load. The maximum displacements of the pile head C1 are 2.1 mm and 1.8 mm while the pile head C2 has the maximum lateral displacements equal to 2.9 mm and 2.3 mm for load patterns 1 and 2, respectively. The displacements of the pile C2 are greater than that of the pile C1 because the diameter of the pile C1 is larger than that of the pile C2. In the other word, the pile C1 is more stiff than the pile C2. However, the pile C2 can carry the maximum lateral load and the measured strains in the longitudinal reinforcement do not reach the yield point. It is implied that the bored pile of staff residence which located near slope can resist the lateral load imposed on the structure during earthquake.

Moreover, the bending curvatures (φ) of the pile C2 can be determined using the data from strain gauges installed on the reinforcing bars. The curvature of the section at each depth is expressed as follows

$$\varphi = \frac{\varepsilon_{s1} - \varepsilon_{s3}}{d_3 - d_1} \qquad (1)$$

where ε_{s1} and ε_{s3} denote the longitudinal strains at each section. d_1 and d_3 denote the distances from the strain gauges to concrete surface in compressive side as shown in Fig. 8. For example, the relationship between the measured strains (ε_{s1} and ε_{s3}) of the section at 0.5 m in depth and lateral load under load pattern 1 are illustrated in Fig. 9. Then using Eq. (1) to calculate the curvatures, the relationship between the curvature and lateral load can be presented in Fig. 10. Figure 11 shows the bending curvatures of pile C2 for both load patterns along the different depths of pile while the maximum lateral load 65 kN is applied. It is seen that the curvature has a maximum value at a depth of 0.50 m and decays rapidly with the depth of the pile. Moreover, the bending moment of pile can be computed from the curvature which be discussed in the next section.

DOI:10.4186/ej.2022.26.3.29

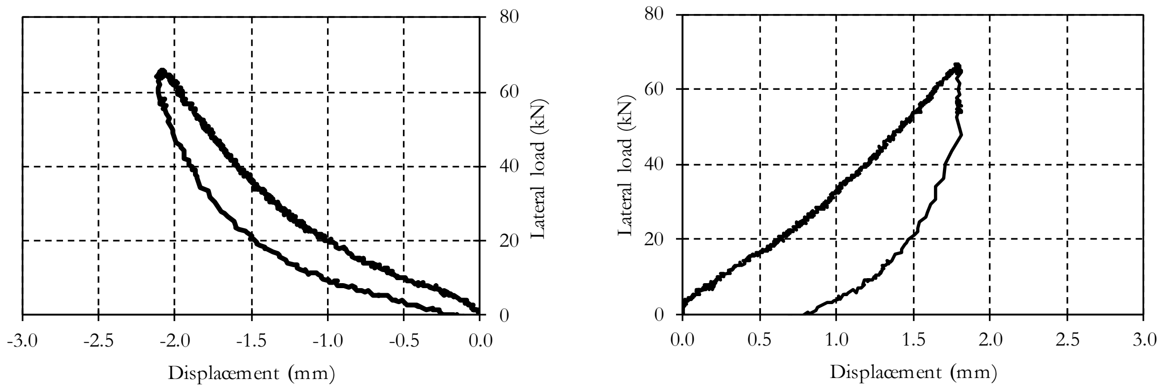

(a) Load pattern 1 (b) Load pattern 2

Fig. 6. Lateral load and pile head displacement relationships for pile C1.

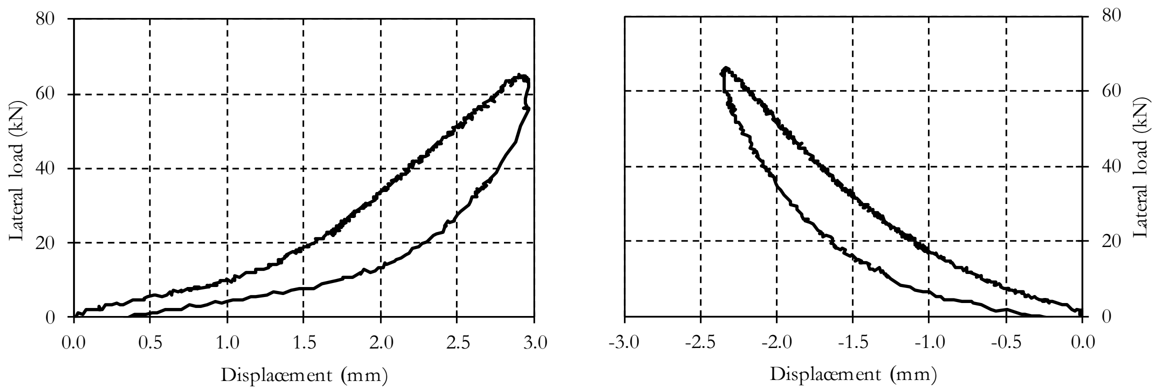

(a) Load pattern 1 (b) Load pattern 2

Fig. 7. Lateral load versus pile head displacement relationships for pile C2.

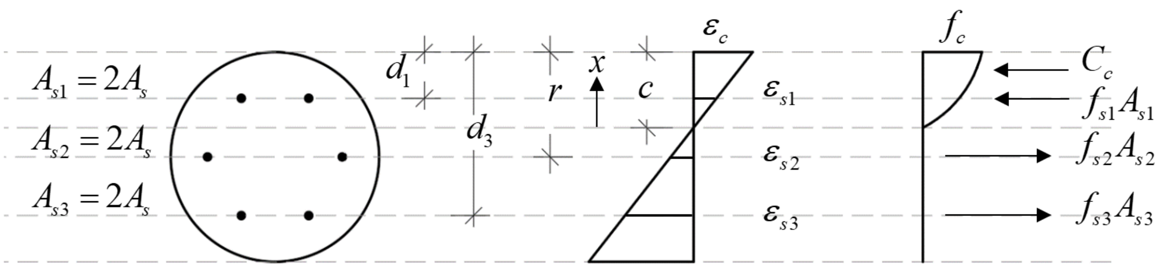

Fig. 8. Strain and stress diagrams of pile section.

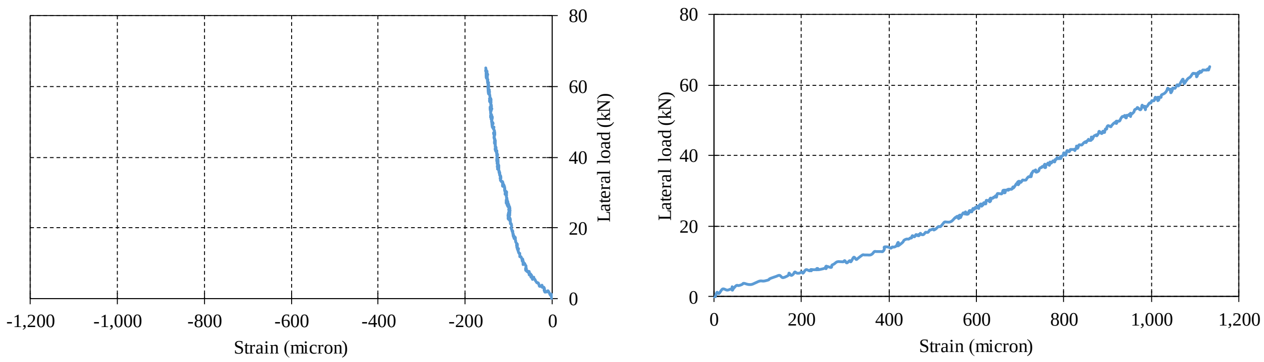

(a) Strain e_{s1} (b) Strain e_{s2}

Fig. 9. Strain curve measured at depth of 0.50 m of pile C2 under load pattern 1.

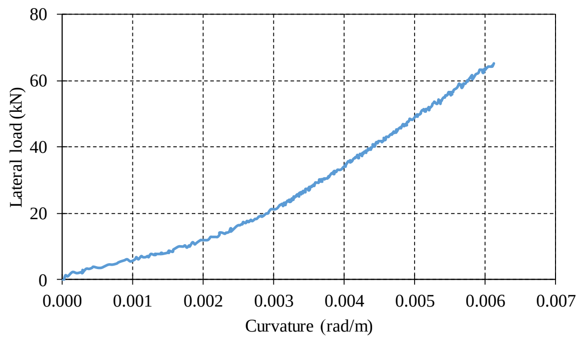

Fig. 10. Curvature of pile C2 section at depth of 0.50 m under load pattern 1.

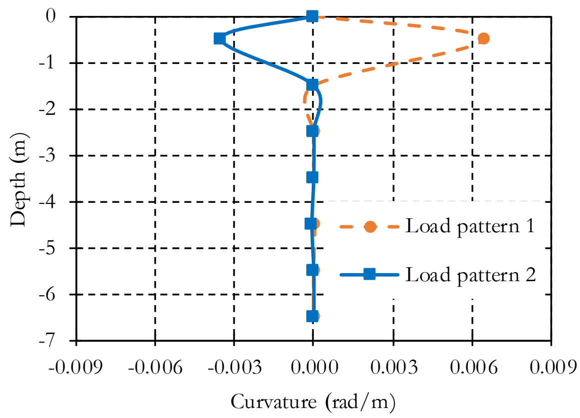

Fig. 11. Curvatures of pile C2 at maximum load 65 kN.

4. Bending Moment- Curvature Relationship

Form the elastic theory of frame member, bending moment and curvature are related as follows

$$M = \varphi EI \quad (2)$$

where M denotes bending moment and EI denotes flexural rigidity. From the Eq. (2), the flexural rigidity of the pile is the slope of bending moment and curvature curve from section analysis as the following steps. First step, let the strain at compressive surface (ε_c) of the pile be a value less than ultimate strain which is equal to 0.003. Second step, assume compressive zone in concrete (c) or location of neutral axis and determine the bending curvature (φ) at the distance from the compressive surface as shown in Fig. 7 from

$$\varphi = \frac{\varepsilon_c}{c} \quad (3)$$

Next step, calculate strain and compressive force in the concrete**.** Strain at a distance x from neutral axis **(**ε_{cx}) can be obtained from Eq**.** **(4)** and stress in concrete **(**f_{cx}) can be calculated using concrete model proposed by Hognestad [18] as shown in Eq**.** **(5).** Then, the compressive force is calculated by integrating the product of the stress and compressive area from $x = 0$ to c as shown in Eq**.** **(6).**

$$\varepsilon_{cx} = \varphi x \quad (4)$$

$$f_{cx} = f_c' \left[\frac{2\varepsilon_{cx}}{\varepsilon_0} - \left(\frac{\varepsilon_{cx}}{\varepsilon_0} \right)^2 \right] \quad (5)$$

$$C_c = \int_0^c dC_c = \int_0^c f_{cx} 2\sqrt{r^2 - (r - c + x)^2}\, dx \quad (6)$$

Then, determine strain and force in the longitudinal steel bars. The strain values occurring each layers of the bars (ε_{si}) depends on the effective depth (d_i) which measured from the compression surface of concrete to the bar i^{th} layer as shown in Eq. (7). Moreover, stress in the reinforcing bar is determined using relationship between stress and strain. The modulus of elasticity of steel (E_s) as shown in Eq. (8) is equal to 200 GPa under conditions of elastic deformation. Force occurring in the bars for each layers (F_{si}) is calculated by the product of the stress (f_{si}) and area of the bar (A_{si}) as in Eq. (9).

$$\varepsilon_{si} = \varphi(c - d_i) \quad (7)$$

$$f_{si} = E_s \varepsilon_{si} \le f_y \quad (8)$$

$$F_{si} = f_{si} A_{si} \quad (9)$$

After that, axial force can be determined simply by summation of compressive and tensile forces as the following

$$P = C_c + \sum F_{si} \quad (10)$$

If the calculated axial force from Eq. (10) is not equal to applied axial load. The process will be repeated by assuming the new compressive zone in second step until the axial force from Eq. (10) is equal to applied axial load. Finally, the bending moment about the central of concrete section is given by

$$M = \int_0^c (r - c + x) dC_c + \sum F_{si} (r - d_i) \quad (11)$$

At the end, the bending moment for each the curvature can be calculated from the first step to the end process. Repeat the process by slightly increasing the compressive strain (ε_c) until the ultimate compressive strain in concrete, i.e. $\varepsilon_c = \varepsilon_u = 0.003$. As a result of the process, the relationship between bending moment and the curvature of plie section can be obtained.

This study considers only the cross-section of pile C2 which has a cross-section as shown in Fig. 3. The reinforcing bars have eccentric from concrete section and as a consequence, the relationships between the bending moment and the curvature under loading pattern 1 and pattern 2 are different. Load pattern 1 will cause counterclockwise bending moments, while load pattern 2 produces a clockwise bending moment. In the experiment, the pile C2 is applied only the lateral force and no axial force, therefore the axial force P in Eq. (10) is equal to zero. The analysis results are shown in Figs. 12 and 13 and the flexural rigidities are obtained from the gradient of bending moment-curvature relationship. It is found that the flexural rigidity (EI) under loading pattern 1 is about 2,349 kN-m² while the flexural rigidity (EI) under loading pattern 2 is, higher, about 3,914 kN-m² .

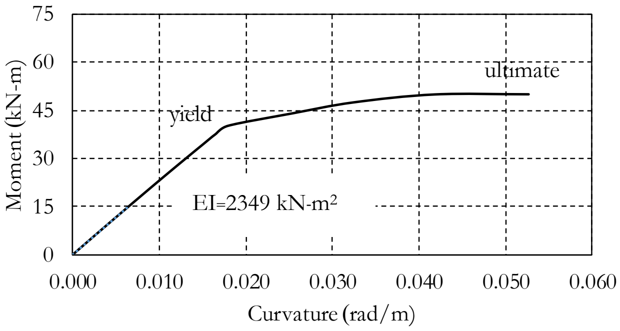

Fig. 12. Bending moment and curvature relation of pile C2 section under loading pattern 1.

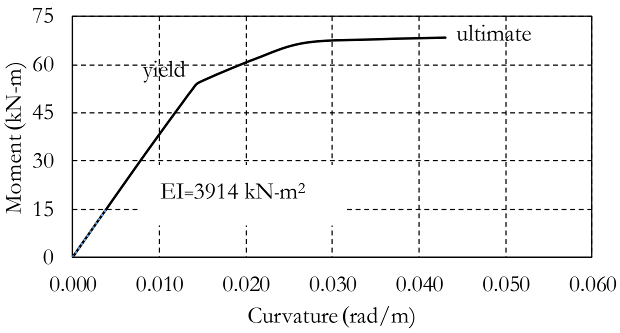

Fig. 13. Bending moment and curvature relation of pile C2 section under loading pattern 2.

To validate the section analysis method, the curvature and the strains of reinforcing bars (ε_{s1} and ε_{s3}) from the analysis as described above are compared to the test results as shown in Figs. 14 and 15. It is found that the analysis results are very well agreed with the experiment. Hence, the bending moment of pile can be approximated by multiplying the measured curvatures (Fig.11) by flexural rigidities (EI) as shown in Fig. 16. It is found that the maximum bending moment is around 15 kN-m that is very conservative comparing to the ultimate moments shown in Figs. 12 and 13.

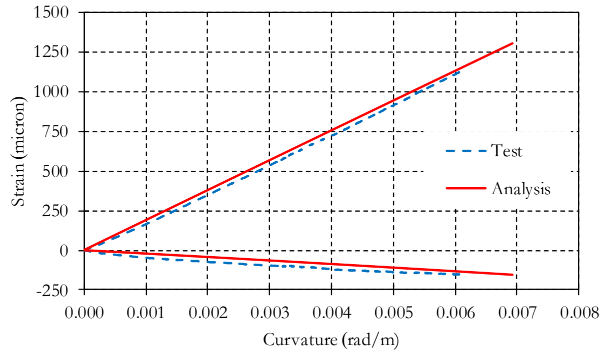

Fig. 14. Comparison of strain values from test at depth of 0.5 m and section analysis under loading pattern 1.

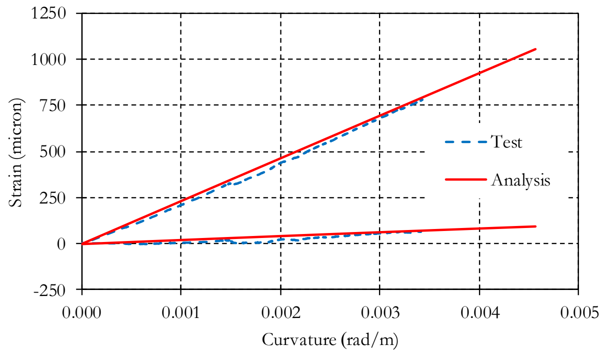

Fig. 15. Comparison of strain values from test at depth of 0.5 m and section analysis under loading pattern 2.

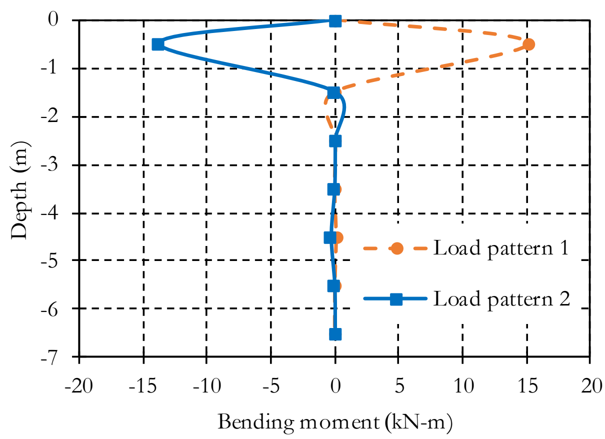

Fig. 16. Approximated bending moment of pile C2 at maximum load 65 kN.

However, the pile discussed in test results is not subjected to vertical load but in fact the pile has to carry the vertical load from the self- weight of structural members and live load as well. The vertical load will increase the flexural rigidity of pile section and the ultimate moment capacity. For example, if the vertical load is about 200 kN, the relationship between bending moment and the curvature is shown in Fig. 17. Flexural rigidities are 20,000 kN- m² and 3,787 kN- m² for uncracked and cracked section, respectively. The cracking moment is about 19 kN- m and the moment capacity is about 89 kN- m. Since it is very difficult to setup vertical load in experiment, the effect of vertical load will be studied by model analysis described in the next section.

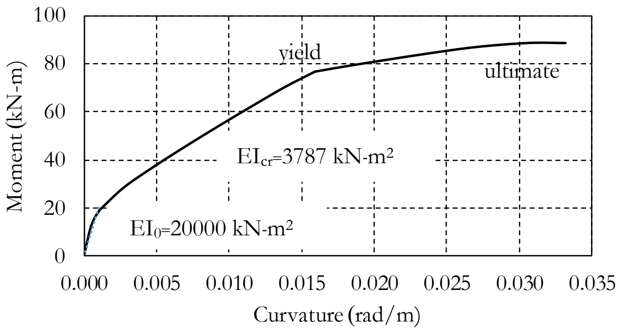

Fig. 17. Bending moment and curvature relation of pile C2 section under lateral loading pattern 2 and vertical load of 200 kN.

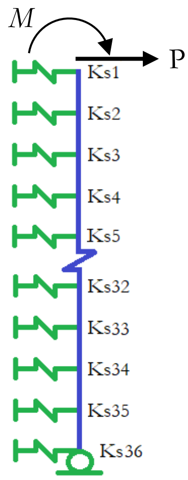

Fig. 18. Structural pile modeling.

5. Laterally Loaded Pile Model Analysis

5.1. Analysis Modeling

The pile is modeled using frame elements and the flexural rigidity (*EI*) of frame elements is obtained from the moment-curvature relationship as presented in the previous section. In this study, the actual pile length will be discretized in 35 elements for all cases. Each element is assigned horizontal springs to represent the soil reactions along the length of the pile and the lateral load and moment is applied on pile head as shown in Fig. 18. In the past, if spring stiffness is assigned to inappropriate value, the analysis cannot capture lateral pile deflection and bending moment of the piles [19]. Davisson [20] recommended the horizontal spring stiffness to represent the clay surrounding pile foundation as

$$K_s = 67 s_u \quad (12)$$

where K_s and s_u denote spring stiffness and undrained shear strength, respectively. Equation (12) is widely used to design pile foundation in Thailand [15]. Because Eq. (12) is proposed for a long time and it is not specified for driven piles or bored piles, the coefficient value of 67 is reconsidered by validate the analysis results with the experimental results from previous researches and this study. Generally, design of structural pile involves the strength of pile structures and the strength of soil surrounding pile. Because the safety factor in geotechnical engineering is about 2.5-3.0, therefore, this study emphasizes on the elastic responses of pile.

5.2. Validation of Analysis Modeling

The test results reported by Chaosittichai and Anantanasakul [8], Nimityongskul et al. [12] and Xu et al. [21] are selected to validate the analysis results. Nimityongskul et al. tested the driven steel pipe piles near slope. The nominal diameter of piles was 305 mm and the length of piles in soil was 7.92 m. The flexural rigidity of piles was 34,875 kN-m². The lateral load was applied at 0.91 m above ground level. The undrained shear strength profile was reported. The average values of undrained shear strength were about 153 kPa for depth of 0-1 m and 68 kPa for the other depth. The pile is modelled and there are lateral load *P* and bending moment M= 0.91P applied at pile head (ground level) (See Fig. 18). It should be noted that the displacement at 0.91 m above ground level can be obtained from calculated pile head displacement at ground level plus 910θ (unit in mm) where θ is the rotation of pile at ground level. Using soil stiffness following Eq. (12) in the analysis, the lateral load and displacement curve (at 0.91 m above ground level) from analysis is well agreed with the tested curves of elastic zone as shown in Fig. 19. Chaosittichai and Anantanasakul [8] also tested three driven steel pipe piles in the soft clay of Bangkok, Thailand. The inner diameter of piles was 250 mm and the thickness was 9 mm. The length of piles in soft soil was 12.5 m. The flexural rigidity of piles was 21,000 kN-m². The undrained shear strength was reported and the average value was about 30 kPa. The soil stiffness from Eq. (12) is used in the analysis and it is found that the displacement is well predicted in elastic zone as seen in Fig. 20. It seems that the soil spring recommended by Davisson [20] can be used in elastic design for driven piles.

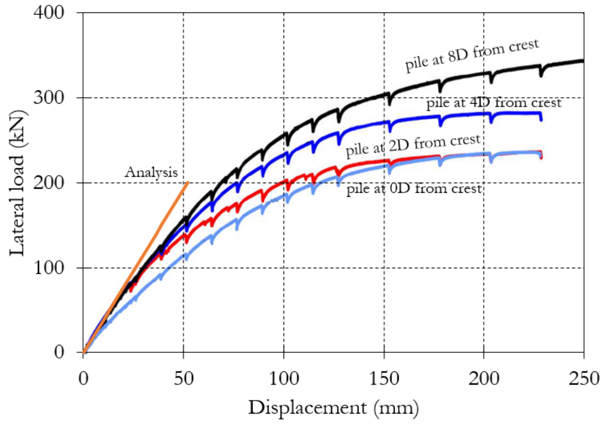

Fig. 19. Load-diaplacment curves of piles studied by Nimityongskul et al. [14].

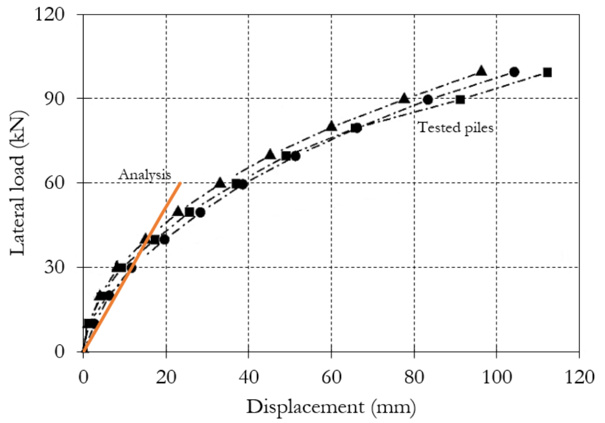

Fig. 20. Load-diaplacment curves of piles studied by Chaosittichai and Anantanasakul [8].

Xu et al. [21] reported the test results of reinforced concrete piles in stiff-to-hard clay studied by Reuss et al. [22] and Liang et al. [23]. Reuss et al. [22] presented full-scale RC piles of Pyramid building, Memphis. The diameter of pile was 0.40 m and the length of pile was 22 m. The initial flexural rigidity of pile section was 51.9 MN-m². Liang [23] presented full-scale shaft with diameter of 1.22 m and length of 10 m. Xu et al. [21] summarized the soil properties as shown in Table 1 and reported the initial flexural rigidity to be 3.26 MN-m². If the soil spring stiffness from Eq. (12) is used in each soil layer for model analysis, it is found that the predicted displacement is very overestimated. The coefficient of 67 in Eq. (12) should be reconsidered for drilled piles. Based on the test results reported by Reuss et al. [22] and Liang [23], the proper coefficient to obtain soil spring stiffness should be 200 instead of 67. Figures 21-22 illustrate the lateral load and pile head displacement curves from analysis and experiments of Reuss et al. [22] and Liang [23], respectively. It is seen that using the soil spring stiffness equal to $200s_u$ can predicted pile head displacement in elastic zone well.

Table 1. Soil properties used for Reuss et al. and Liang cases.

Case	Layer thickness (m)	Soil description	s_u (kPa)
Reuss et al.	1.8	Gravelly clay	67
	11.3	Soft silty clay	29
	6.8	Soft to stiff clay	30
	2.1	Stiff to hard clay	72
Liang	0.9	Silt, clay	220
	0.9	Silt, clay	241
	1.2	Clay shale	311
	1.6	Clay shale	690
	1.4	Clay shale	1033
	4.0	Clay shale	2067
	2.0	shale	2067

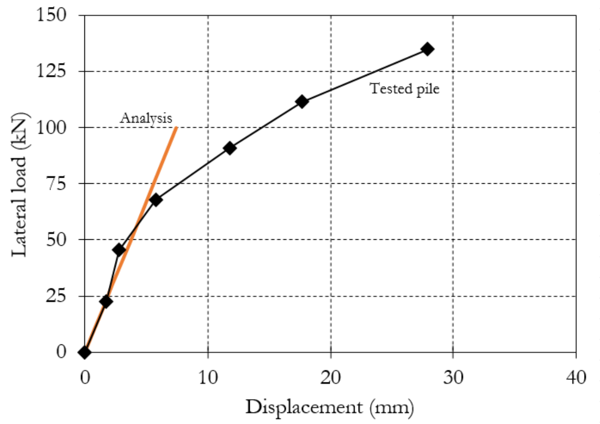

Fig. 21. Load-diaplacment curves of piles studied by Reuss et al. [22].

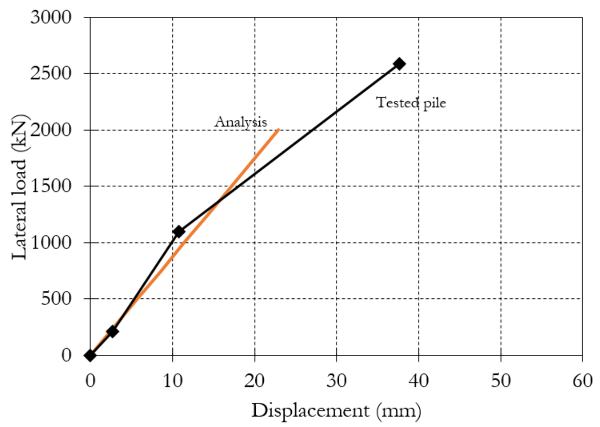

Fig. 22. Load-diaplacment curves of piles studied by Liang [23].

The elastic analysis has limitation depended on the surrounding soil stress and the change of flexural rigidity. The surrounding soil stress σ_s of each layer can be obtained from spring force as

$$\sigma_s = \frac{K_s \Delta}{Dh} \tag{13}$$

where Δ is lateral displacement of soil spring, D is diameter of pile and h is length of frame element. Based the analysis results, the elastic lateral load is limit when the surrounding soil stress σ_s develop to $2s_u - 2.5s_u$. The change of flexural rigidity usually occurs in RC piles. As shown in Fig. 17, the RC pile after crack appear has reduced flexural rigidity. If the bending moment in pile is more than cracking moment, the flexural rigidity using in analysis model should be updated to cracked flexural rigidity.

5.3. Analysis of Tested Pile and Effect of Vertical Load

The soil properties at the staff residence building site were investigated before construction as shown in Table 2. During soil drilling for pile construction, it is not observed the water in holes. This implies that the water table is below the piles. In this study, Kunzelstab Penetration Test (KPT) in accordance with DIN 4049 standard is also conducted on the pile-test site. The number of blows is recorded every penetration depth of 20 cm of cone. In Thailand, Electricity Generating Authority of Thailand (EGAT) performed extensive field tests to establish the equation to predict ultimate bearing capacity from KPT [24]. The proposed equations for clay are

$$N' = \begin{cases} N & ,N \le 15 \\ 15 + 0.5(N - 15) & ,N > 15 \end{cases} \tag{13}$$

$$Q_u = 18.84(N' + 0.954) \text{ (kPa)} \tag{14}$$

These equations are currently used for design the foundation of electric pole in mountainous rural areas of Thailand, although it was studied for long time ago since 1980. The ultimate bearing capacities at various depths determined from N and N' values from KPT results are shown in Table 3. Then, the undrained shear strength can be approximated about half of ultimate bearing capacity. It is seen that the estimated undrained shear strengths from KTP conform to the soil boring test.

As described in the previous section, the tested pile C2 has flexural rigidities of 2,349 kN-m^2 and 3,914 kN-m^2 for the load pattern 1 and pattern 2, respectively. The head lateral displacements at maximum load (65 kN) of the pile C2 are 2.90 mm and 2.30 mm for load pattern 1 and pattern 2, respectively. If the soil spring stiffness is assigned to $200s_u$, the predicted displacements are equal to 2.63 mm and 2.39 mm that are acceptable with the test results. Figure 23 presents the analytical bending moment diagram of the pile C2 at maximum lateral load. The maximum values of bending moment are observed at 0.50 m in depth and it decreases rapidly along the pile approaching negligible level when the depth more than 4 m both load patterns. It is should be noted that the inflection points of two different lateral load patterns occur at 2.0 m in depth of pile. The maximum bending moment values are equal to 9.80 kN-m and 11.4 kN-m corresponding to the pile flexural rigidities of 2,349 kN-m^2 and 3,914 kN-m^2, respectively. As shown in Fig. 16, the maximum bending moments from experiment are 14.40 kN-m and 13.40 kN-m. which are approximately 1.30 times greater than the analytical results. This is acceptable value that the pile foundation is required to be 2.50 of safety factor. The analyses in cases of Chaosittichai and Anantanasakul, Nimityongskul et al. and Reuss et al. are also observed that the values of bending moment from test is greater than the analysis results about 1.3-1.4 times.

Table 2. Soil properties at the staff residence building site.

Depth (m)	**Soil description**	s_u **(kPa)**
1.5	Lean clay-Lean silt	152
2.0	Lean clay-Lean silt	241
2.5	Lean clay-Lean silt	329
3.0	Lean clay-Lean silt	366
3.7	Lean clay-Lean silt	402

Table 3. Ultimate bearing capacities determined from KPT results.

Depth (m)	N **(blows/0.2 m)**	N' **(blows/0.2 m)**	Q_u **(kPa)**	s_u **(kPa)**
0.20	90	52.5	1007	503
0.40	38	26.5	517	258
0.60	30	22.5	442	221
0.80	49	32.0	621	310
1.00	83	49.0	941	470
1.40	48	31.5	611	305
1.80	47	31.0	602	301
2.00	62	38.5	743	371
2.20	63	39.0	752	376
2.40	65	40.0	771	385
2.60	62	38.5	743	371
2.80	64	39.5	762	381

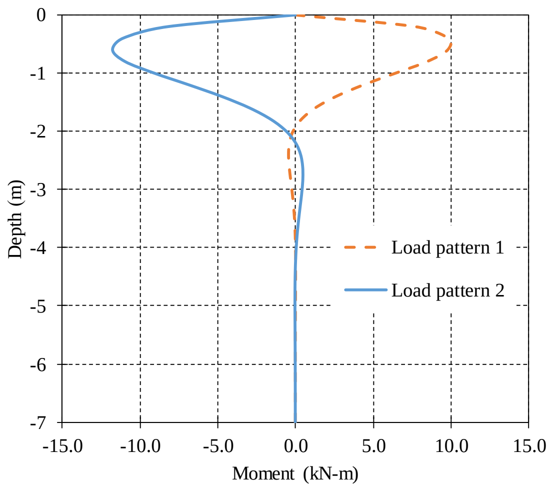

Fig. 23. Bending moment diagram of pile C2 computed in the analyses.

From data shown in experiment and computational model, it is found that the flexural rigidity of pile section (EI) has a significant effect on the lateral load behavior of the pile. The higher value of EI results in less the lateral displacement, more the bending moment and more depth of inflection point. Therefore, the analytical model must be careful to determine the actual flexural rigidity of pile. In addition, the vertical load will affect the flexural rigidity of pile section. For example, the pile subjected to vertical load of 200 kN has initial flexural rigidity of 20,000 kN-m^2. When this flexural rigidity is used in the analysis of pile with the lateral load of 65 kN, the maximum displacement at the pile head decrease to 1.70 mm and the maximum bending moment increase to 19.72 kN-m at a depth of 0.80 m as shown in Fig. 24. The inflection point occurs at depth of 3.40 m. However, the maximum stress value in reinforcing bar is less than yield strength.

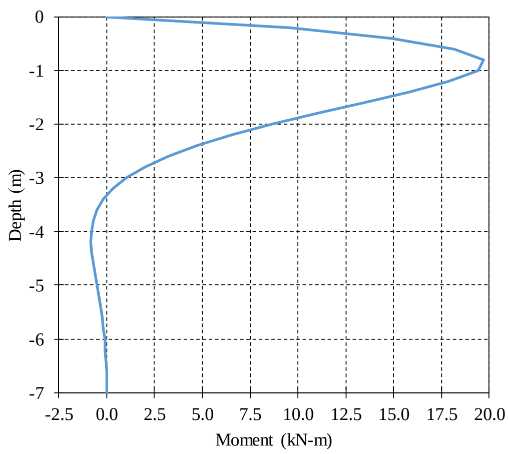

Fig. 24. Bending moment of the pile C2 from analysis with EI equal to 20,000 kN-m^2.

6. Conclusion

From field lateral pile load test and the comparison with the analysis results, it can be concluded that test piles which has detailing construction drawing of staff residence, University of Phayao can be transfer the earthquake equivalent lateral force base shear to soil medium. It is known from the strength of longitudinal reinforcement is not to exceed the yielding strength, even though the pile is located near slope.

In this study, spring stiffness model is validated with the test results in elastic zone from previous researches. The stiffness of $K_s = 67s_u$ recommended by Davisson [20] can well predict the displacement of driven piles but it is very overestimated for RC bored piles. For bored piles, the soil spring stiffness of $K_s = 200s_u$ should be used to predict the displacement and bending moment. However, lateral displacement and bending moment from these analyses indicate good agreement in the elastic zone. In addition, flexural rigidity of pile has significant impact on the lateral load behavior. The higher value of the flexural rigidity results in less the lateral displacement, more the bending moment and more depth of inflection point.

Acknowledgement

The research is financially supported by University of Phayao. The author is also grateful to Wiangphan Part., Ltd. and D-Engineering Design Co., Ltd who helped in RC bore piles construction.

References

[1] Ministry of Interior (Thailand), "Ministerial regulation—Prescribing load capacity, resistance, and durability of buildings, and bearing capacity of soil supporting buildings in seismic resistance," *Royal Thai Government Gazette*, vol. 138, no. 16a, pp. 13-18, 2021.

[2] S. Prakash and H. D. Sharma, *Pile Foundations in Engineering Practice*. New York: John Wiley & Sons, 1990.

[3] L. C. Reese and W. F. Van Impe, *Single Piles and Pile Groups under Lateral Loading*. London, UK: Taylor & Francis, 2001.

[4] H. S. Chore, R. K. Ingle, and V. A. Sawant, "Parametric study of laterally loaded pile groups using simplified F. E. models," *Coupled Systems Mechanics*, vol. 1, no. 1, pp. 1–7, 2012.

[5] K. B. Ladhane and V. A. Sawant, "Dynamic response of 2 piles in series and parallel arrangement," *Eng. J.*, vol. 16, no. 4, pp. 63-72, Apr. 2012.

[6] A. B. Huang, C. K. Hsueh, M. W. O'neill, S. Chern and C. Chen, "Effects of construction on laterally loaded pile groups," *J. Geotech. Geoenviron. Eng.*, vol. 127, no. 5, pp. 385-397, 2001.

[7] T. Hanich, V. Hristovski, and N. Zurovski, "Lateral load test of reinforced concrete bored piles of bridge eye in skopje," presented at *IZIIS-50 International Conference on Earthquake Engineering and Seismology*, Copenhagen, Denmark, 2015.

[8] G. Chaosittichai and P. Anantanasakul, "Field experimental study of load-deflection behavior of driven piles in soft Bangkok clay," *Kasem Bundit Engineering Journal*, vol. 8, pp. 373-385, 2018.
[9] H. Matlock, "Correlations for design of laterally loaded piles in soft clay," in *Proc., 2nd Annual Offshore Technology Conf.*, Offshore Technology Conference, Houston, 1970, pp. 577–594.
[10] S. V. Sivapriya and S. R. Gandhi, "Experimental and numerical study on pile behaviour under lateral load in clayey slope," *Indian Geotech J*, vol. 43, no. 1, pp. 105–114, 2013.
[11] K. Georgiadis and M. Georgiadis, "Undrained lateral pile response in sloping ground," *J. Geotech. Geoenviron. Eng.*, vol. 136, no. 11, pp. 1489–1500, 2010.
[12] K. Muthukkumaran and N. A. Begum, "Experimental investigation of single model pile subjected to lateral load in sloping ground," *Geotech. Geol. Eng.*, vol. 33, pp. 935–946, 2015.
[13] N. A. Begum and K. Muthukkumaran, "Experimental investigation on single model pile in sloping ground under lateral load," *Int. J. of Geotech. Eng.*, vol. 3, no. 1, pp. 133-146, 2009.
[14] N. Nimityongskul, Y. Kawamata, D. Rayamajhi and S. A. Ashford, "Full-scale tests on effects of slope on lateral capacity of piles installed in cohesive soils," *J. Geotech. Geoenviron. Eng.*, vol. 144, no. 1, p. 04017103, 2018.
[15] A. Pimanmas, P. Chaimahawan, and P. Joyklad, "Advanced structural design of reinforced concrete footing," Civil Engineering Consultant and Training Co., LTD., Bangkok, Thailand, 2012.
[16] *Thai Industrial Standard-Steel Bars for Reinforced Concrete: Deformed Bars*, TIS 24-2559, Ministry of Industry, Bangkok, Thailand, 2016.
[17] *Thai Industrial Standard-Steel Bars for Reinforced Concrete: Round Bars*, TIS 20-2559, Ministry of Industry, Bangkok, Thailand, 2016.
[18] J. K. Wight and J. G. MacGregor, "Materials," in *Reinforced Concrete: Mechanics and Design*, 6th ed. Pearson, 2011, ch. 3, sec. 3.14, pp. 59-66.
[19] A. Rahmani, T. Mahdi, W. L. D. Finn, and C. E. Ventura, "Evaluation of p-y springs for nonlinear static and seismic soil-pile interaction analysis under lateral loading," *Soil Dynamics and Earthquake Engineering*, vol. 115, pp. 438-447, Dec. 2018.
[20] M. T. Davisson, "Lateral load capacity of piles," *Highway Research Record*. Washington, DC, 1970, pp. 104-112.
[21] L.-Y. Xu, F. Cai, Fei, G.-X. Wang, G.-X. Chen, and Y.-Y. Li, "Nonlinear analysis of single reinforced concrete piles subjected to lateral loading," *KSCE J. of Civ. Eng.*, vol. 21, no. 7, pp. 2622-2633, 2017.
[22] R. Reuss, S. T. Wang and L. C. Reese, "Tests of piles under lateral loading at the pyramid building, memphis, Tennessee," *Geotechnical News*, vol. 10, no. 4, pp. 44-49, 1992.
[23] R. Y. Liang, "Pressure meter to predict the lateral load capacity of drilled shafts on slopes," A research report submitted to the Ohio Department of Transportation and FHWA.
[24] EGAT, "Soil exploration by Kunzelstab penetration test," Electricity Generating Authority of Thailand, 1980.

Wichairat Kaewjuea, photograph and biography not available at the time of publication.

Somboon Shaingchin, photograph and biography not available at the time of publication.

Wittawat Khamtip, photograph and biography not available at the time of publication.

Thanakorn Chompoorat, photograph and biography not available at the time of publication.

Preeda Chaimahawan, photograph and biography not available at the time of publication.